Available online at www.sciencedirect.com
SCIENCE DIRECT®
Surface Science 529 (2003) 1–10
SURFACE SCIENCE
www.elsevier.com/locate/susc

X-ray standing wave study of Si/Ge/Si(0 0 1) heterostructures grown with Bi as a surfactant

W. Rodrigues [a,b], B.P. Tinkham [c], O. Sakata [c], T.-L. Lee [c], A. Kazimirov [c], M.J. Bedzyk [b,c,*]

[a] Department of Physics, Northwestern University, Evanston, IL 60208, USA
[b] Argonne National Laboratory, Argonne, IL 60439, USA
[c] Materials Science Department and Materials Research Center, Northwestern University, Cook Hall, Evanston, IL 60208, USA

Received 1 November 2002; accepted for publication 8 February 2003

Abstract

X-ray standing wave (XSW) analysis was used for an atomic-scale structural study of ultra-thin Si/Ge heterostructures grown on Si(0 0 1) by surfactant mediated epitaxy with Bi as the surfactant. XSW measurements were performed for the Si(0 0 4) and Si(0 2 2) Bragg reflections for Ge coverages from 1 to 10 monolayers. The measured Ge coherent positions agree with the calculated Ge positions for a tetragonally distorted Ge lattice formed on Si(0 0 1) using continuum elasticity theory. However, the measured Ge coherent fractions are smaller than expected. The quality of the Si cap layer and its registry with the underlying Si(0 0 1) substrate lattice was also determined by combining the XSW technique with evanescent-wave emission.
© 2003 Elsevier Science B.V. All rights reserved.

Keywords: Epitaxy; Germanium; Silicon; Bismuth; Surface defects; Growth; X-ray standing waves

1. Introduction

Starting with the first reported growth of semiconductor heterostructures by surfactant mediated epitaxy (SME) [1], it has been established that the surfactants serve to alter the growth kinetics by saturating the dangling bonds at the growth surface [1,2]. For the case of Ge/Si heterostructures, the lattice mismatch is 4% and Ge has a lower surface energy than Si. Although Ge will wet the Si(0 0 1) surface, it is well known that after about 3 monolayers of growth Ge islands begin to form to relieve the build up of strain energy [3]. For Si growth on Ge, the lower surface energy of Ge results in its segregation into the Si. These limitations prevent the growth of suitable Ge/Si based superlattice structures. However, SME has been used to prevent the early onset of islanding and force layer-by-layer growth by inhibiting diffusion of Ge adatoms [4]. SME has also been used to prevent Ge segregation into Si and to improve the abruptness of the Ge–Si interface [5]. The tetragonal distortion of Ge lattice due to the

* Corresponding author. Address: Materials Science Department and Materials Research Center, Northwestern University, Cook Hall, Evanston, IL 60208, USA. Tel.: +1-847-491-3570; fax: +1-847-467-2269.
E-mail address: bedzyk@northwestern.edu (M.J. Bedzyk).

0039-6028/03/$ - see front matter © 2003 Elsevier Science B.V. All rights reserved.
doi:10.1016/S0039-6028(03)00303-0

lattice mismatch between Ge film and Si substrate can be expected to influence the vertical and in-plane ordering in different ways. By imposing kinetic barriers, surfactants are understood to improve the in-plane ordering by reducing the adatom diffusion length. How the vertical ordering of atoms is affected by surfactants is less clear. To realize improved device performance from Ge/Si based superlattice structures, it is important to understand the nature of strain and disorder both in-plane and out-of-plane.

Compared to other techniques, X-ray based techniques have several advantages for investigating strain and disorder in materials. These include elemental sensitivity, and the ability to directly and non-destructively measure strain in buried layers. Although several groups have investigated strain in Ge grown on Si(0 0 1) [6], to our knowledge there is no study reported about the disorder in metastable Si/Ge/Si(0 0 1) structures grown by SME.

Most of the surfactants used in semiconductor SME are from groups IV, V, and VI of the periodic table and As and Sb are the most studied surfactants [1,2,4,6–8]. Arsenic has been effective in growing relatively thick, 2-D pseudomorphic Ge films on Si(0 0 1) [4], however, it is easily incorporated into the epitaxial structures and may act as a dopant. This can significantly change the electrical properties of the films. Sb has been shown to promote formation of 3-D Ge islands at higher temperatures [2] and is very difficult to be removed from the surface [7]. Several groups have reported the use of Bi as a surfactant on (0 0 1) surfaces [9–13]. Using ion scattering and TEM Kawano et al. concluded that 1 ML of Bi pre-deposited on Si(0 0 1) enabled the growth of high quality crystalline Ge epilayers (~20 nm thick) with a smooth surface and relatively few defects [9]. They note that the same Ge films grown without Bi resulted in an island structure. A more recent study investigated Bi and Sb as surfactants and pointed out the dependence of Ge crystal quality on Sb and Bi coverage [11]. Bi has also been shown to be effective in growing smooth, relaxed layers on Si(1 1 1) substrates [14], and was also found to be effective in growing metastable, pseudomorphic SnGe/Ge(0 0 1) heterostructures [12]. Bi appears to lack the aforementioned inadequacies of both As and Sb. In this paper we report the evolution of disorder in Bi-mediated SME grown Si/Ge/Si(0 0 1) heterostructures using the X-ray standing wave (XSW) technique. To the authors' knowledge there have been no reported studies that have evaluated the registry of both the Ge and Si epitaxial layers in the same structure with respect to the Si(0 0 1) substrate using XSW.

2. Experimental

The samples were prepared by molecular beam epitaxy (MBE) in an ultra-high vacuum (UHV) chamber with a base pressure of 1×10^{-10} Torr. The samples were degreased and Shiraki etched before being introduced in the chamber. Samples were then out-gassed for at least 12 h at 650 °C and then annealed at 950 °C to achieve a clean Si(0 0 1) surface, which was verified by a sharp 2-domain 2×1 LEED pattern. No oxygen or carbon contamination of the surface was observed by Auger electron spectroscopy (AES). Samples were prepared with Bi as a surfactant with Ge coverages ranging from 1 to 10 ML. Throughout the growth, the temperature of the sample was held at 400 °C. Initially, 1 ML of Bi was deposited and then Ge deposition was carried out at a rate of 0.06 ML/min by evaporation from a Knudsen cell. During the Ge growth, a constant overpressure of Bi was maintained to compensate for thermally induced Bi desorption. After Ge deposition was complete Si deposition was carried out at a rate of about 1 ML/min from an e-beam evaporator. In order to prevent Ge segregation into the Si cap and thereby achieve an abrupt interface transition, the Bi flux was not turned off until ~20 ML of the silicon cap had been deposited. The nominal thickness of the deposited Si was 100 Å. For the sake of comparison a sample with 1 ML of Ge without Bi was also prepared. The absolute Ge coverage of each sample was measured by comparing its Ge Kα fluorescence yield to that of a standard sample that was calibrated by Rutherford back-scattering. At each stage of the film deposition, the surface was studied by LEED and AES at room temperature.

Bi has very low solubility in both Ge and Si and its surface free energy is lower than either Si or Ge.

Bi belongs to group V and can saturate the dangling bonds at the Si or Ge(0 0 1) surface. The saturation of Si or Ge dangling bonds reduces the surface energy and therefore Bi termination of the surface is energetically favored. These properties suggest that Bi strongly segregates into both Si and Ge and floats to the surface; this is an important prerequisite for a surfactant to be effective. The surface reconstruction of Bi on Si(0 0 1) is coverage dependent. The LEED pattern after Bi deposition on Si at 400 °C was 2-domain $(2 \times n)$ with n equal to 4 or 5. The saturation coverage is then equal to $(n-1)/n$ ML which is approximately 0.8 ML based on previous measurements [15]. The LEED pattern after Ge deposition over Bi was found to be similar with weaker nth order spots resulting from small fraction of Bi leaving the surface. The intensity of the Bi Auger peak did not change after Ge deposition. Similar surface conditions were observed after Si deposition, however the features in the LEED pattern were more diffuse.

The XSW measurements were performed at the 5ID-C beamline at the Advanced Photon Source in open air. In the XSW technique [16] a monochromatic X-ray beam is tuned to a Bragg reflection of the crystal sample. The interference of the incident and the reflected beam produces a XSW field in and above the crystal. The periodicity of the XSW field is same as the diffracting lattice planes. The phase υ of the reflected beam with respect the incident beam shifts by 180° as the Bragg angle θ is scanned from low-angle side to high-angle side of the rocking curve. This causes the antinodes of the XSW field to shift inwards by one-half of the d-spacing d_{hkl}. The shifting XSW field modulates the fluorescence yield. This yield is formulated as:

$$Y(\theta) = 1 + R(\theta) + 2\sqrt{R(\theta)} f_H \cos[v(\theta) - 2\pi P_H],$$

where $R(\theta)$ is the reflectivity of the diffracted beam. Parameters f_H (coherent fraction) and P_H (coherent position) are the amplitude and phase, respectively, of the $\boldsymbol{H} = hkl$ Fourier component of the spatial distribution of the fluorescent atoms. The model independent parameters, f_H and P_H, along with their respective error bars are determined from the weighted chi-square fit of the above yield equation to the data.

For the XSW measurement of the Ge buried layer, the X-ray energy was tuned to 12.5 keV and the Ge Kα fluorescence was collected by a Si (Li) solid state detector. For the measurement of the Si capping layer, the energy was changed to 8.0 keV in order to eliminate the Ge K fluorescence signal and to enhance the 1.74 keV Si Kα fluorescence. The Si XSW experiment was performed in a helium atmosphere in order to reduce air absorption of the Si fluorescence as well as eliminate Argon fluorescence from the spectrum. The evanescent-wave emission technique [17,18] (that collects the X-ray emission at a take-off angle α smaller than the critical angle α_c for total external reflection) was used to discriminate against Si K fluorescence originating from the Si substrate. Referring to the inset in Fig. 1; based on Snell's law, the index of refraction for X-rays being smaller than unit causes the internal angle α' for an escaping photon to be smaller than the external angle α. At $\alpha < \alpha_c$, the real part of $\alpha' = 0$ and an evanescent-wave emission condition exists in which the escape depth is dramatically reduced. A slit was used in front of the fluorescence detector in order to define range of take-off angle α. The lower limit was aligned with the horizon of the sample surface ($\alpha_l = 0$), and the upper limit (α_u) was defined by a slit parallel to the sample surface and between the sample and fluorescence detector. The "effective" linear

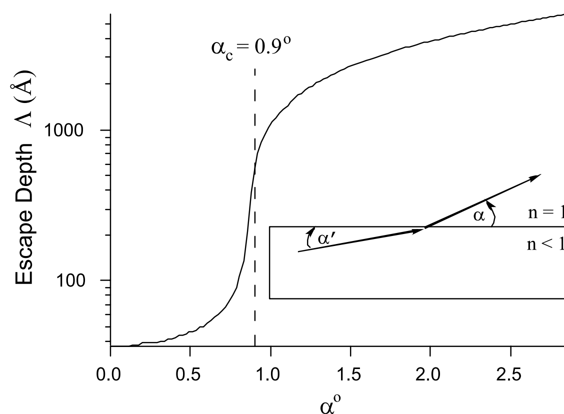

Fig. 1. Escape depth of 1.74 keV Si Kα fluorescence X-rays in Si as a function of take-off angle α. The inset depicts the refraction of an outgoing X-ray as it passes through the interface.

absorption coefficient, μ_z, is related to the index of refraction, $n = 1 - \delta - i\beta$ as:

$$\mu_z(\alpha) = \frac{2\sqrt{2}\pi}{\lambda_2}\left\{\left[(2\delta - \alpha^2)^2 + 4\beta^2\right]^{1/2} + 2\delta - \alpha^2\right\}^{1/2}. \quad (1)$$

λ_2 is the wavelength of the emitted photon. Note that for $\alpha \gg \alpha_c$, $\mu_z = \mu_0/\sin\alpha$. For Si Kα X-rays escaping from a Si substrate with a mirror-like surface, the critical angle is $\alpha_c = \sqrt{2\delta} = 0.9°$. Fig. 1 shows the calculated escape depth $\Lambda = \mu_z^{-1}$ as a function of take-off angle, α. Λ has a minimum value of 36 Å at $\alpha = 0$ and dramatically increases at $\alpha = \alpha_c$. This abrupt reduction in the escape depth due to refraction effects below the critical angle makes this technique surface sensitive.

For our XSW measurement of the 100 Å thick Si cap, it was necessary to eliminate the detection of X-rays from the Si substrate. We ensured this by positioning the upper slit to have a take-off angle just below the critical angle. The (0 0 4) XSW measurements were performed and then repeated after lowering the slit by an additional 0.1°. The absence of any change in the Si P_H and f_H values after changing the slit position proved that the fluorescence from the Si substrate was negligible. The Si capping layer measurements were performed on the 1.6, 3.0 and 3.4 ML Ge coverage samples that were grown with Bi as a surfactant and the 1.1 ML Ge sample grown without Bi.

The coherent fraction depends on three factors: $f_H = Ca_HD_H$. C is the ordered fraction, a_H is the geometrical factor, and $D_H = e^{-M}$ is the Debye–Waller factor. The Debye–Waller (DW) factor takes into account the thermal vibrations of the atoms. For buried epitaxial layers, this term can be estimated using the Debye temperature or it can be measured experimentally. The geometrical factor is the modulus of the geometrical structure factor and takes into consideration the multiple positions the adatoms can take. For a singular position $a_H = 1$ and for multiple positions $a_H < 1$. Therefore, for a single strained monolayer of Ge buried in a Si(0 0 1) matrix a_H is ideally unity, but for coverages greater than 1 ML the Ge atoms should take more than one position relative to the underlying Si lattice and the coherent fraction diminishes. For a defect free pseudomorphic epitaxial film, the geometrical factor should accurately describe the atomic distribution of the layer. For this situation $C = 1$. In the case of an adsorbate layer on a surface values of C less than one imply that a fraction of the adsorbate is incommensurate. In our case of an epitaxial film, crystalline defects will have the effect of lowering the ordered fraction. Assuming a Ge film composed of several atomic layers to be pseudomorphic with a tetragonal distortion of the Ge lattice according to continuum elasticity theory, the Ge coherent fraction for the film can be written as:

$$f_H = C\frac{1}{N}\frac{\sin(N\pi\delta_H^F)}{\sin(\pi\delta_H^F)}D_H, \quad (2)$$

where N is the number of atomic layers in the film and δ_H^F is the relative difference between the tetragonally distorted Ge lattice and the Si substrate lattice for the planes of index H. The coherent position for such a film is given as:

$$P_H = \frac{(N-1)}{2}\delta_H^F + \delta_H^I. \quad (3)$$

δ_H^I in this equation refers to the offset at the Ge/Si interface. More specifically, δ_H^I is the fractional d-spacing offset between the Si(0 0 4) bulk extrapolated atomic plane and the first Ge epitaxial layer plane. We will assume that the Si–Ge atomic layer spacing at the interface is half way between the bulk Si spacing and the Ge–Ge spacing in the strained layer. Thus in this study, we will assume $\delta_H^I = \delta_H^F/2$. From continuum elasticity theory the perpendicular strain ($\varepsilon_\perp$) and the in-plane strain ($\varepsilon_\parallel$) are related by the elastic constants c_{12} and c_{11} as $\varepsilon_\perp = -2(c_{12}/c_{11})\varepsilon_\parallel$. Using $c_{11} = 12.40 \times 10^{10}$ N m^{-2}, $c_{12} = 4.13 \times 10^{10}$ N m^{-2} [19], and $\varepsilon_\parallel = 0.040$ as inputs, continuum elasticity theory predicts that $\varepsilon_\perp = 0.027$ and $\delta_{004}^F = ((a_{Ge} - a_{Si})/a_{Si}) + \varepsilon_\perp = 0.068$. Based on symmetry $\delta_{022} = \delta_{004}/2$.

For the Si atoms in the Si capping layer, the coherent position ideally should be $P_{004}^{Cap} = N\delta_{004}^F$. The coherent fraction for a perfect epitaxial thin film of Si on a Ge terminated Si(0 0 1) substrate should be equal to the Debye–Waller factor for Si. However, the measured value is expected to be slightly lower due to effects such as: the formation of a native SiO_2 layer (typically 20 Å thick) and

defects in the epitaxial Si cap. If the Si cap was grown in tension (underlying Ge partially relaxed) the Si cap coherent fraction would be systematically lower as well.

3. Results

Fig. 2 displays the (0 0 4) XSW Ge data and analysis for a 1.6 ML Ge Si/Ge/Si(0 0 1) sample grown with Bi and a 1.1 ML sample grown without surfactant. The measured Ge coherent positions (see inset of Fig. 2) agree with the continuum elasticity theory prediction shown in Eq. (3). The sample grown with Bi has a higher Ge coverage (1.6 ML) yet has a higher coherent fraction. This result supports the claim that Bi as a surfactant has been effective in improving the epitaxial quality of the strained Ge buried layer. For the full set of Bi-SME grown samples, the model independent XSW measured coherent fraction and coherent position values for Ge as a function of measured Ge coverage are plotted in Fig. 3. For comparison the (0 0 4) and (0 2 2) lines are calculated by using

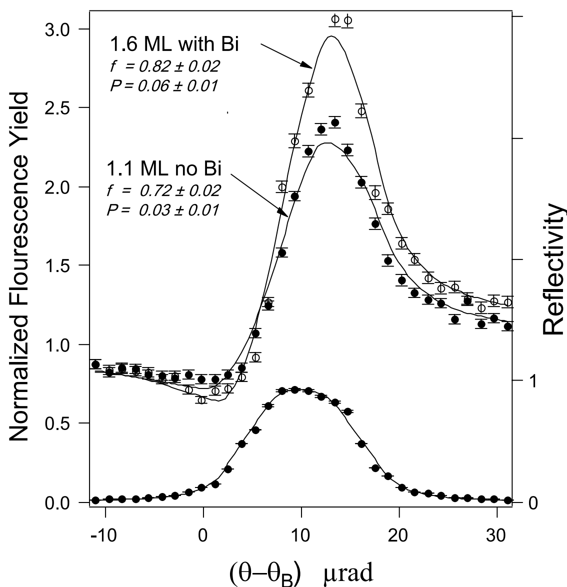

Fig. 2. Angular dependence of (0 0 4) XSW data (markers) and best fit (solid lines) for Ge Kα fluorescence yield and Si(0 0 4) reflectivity for 1.6 ML of Ge with Bi and 1.1 ML without Bi on Si(0 0 1).

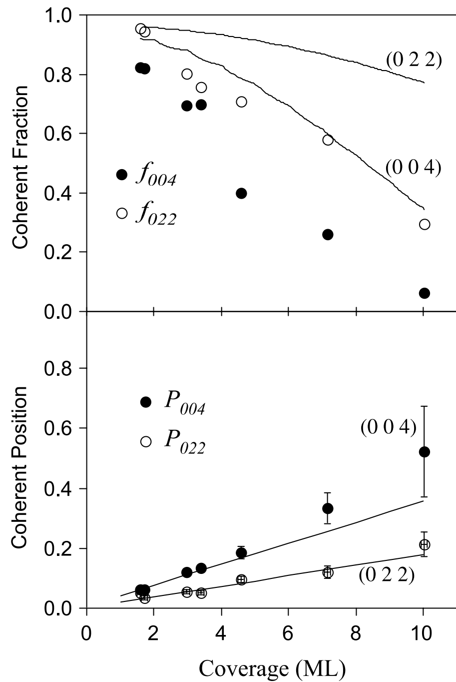

Fig. 3. Measured Ge coherent positions and coherent fractions (dots) for Si(0 0 4) and Si(0 2 2) reflections plotted as function of Ge coverage with Bi as a surfactant. The lines represent Eqs. (2) and (3) calculated (0 0 4) and (0 2 2) coherent fractions and coherent positions using continuum elasticity theory.

continuum elasticity theory and assume that $C = 1$ in Eqs. (2) and (3). As can been seen the calculated positions from this idealized model match the measured positions for both the (0 0 4) and (0 2 2) reflections; especially below 7 ML. The measured coherent fractions, while following the predicted trend, are much lower than the calculated values for the entire range of Ge coverage.

Isotropic variations in the Ge position about its expected position would result in a reduction of measured coherent fraction without changing the measured coherent position. One such effect results from the room temperature thermal vibrations of the Ge atoms. This is already incorporated into Eq. (2) as the thermal DW factor $e^{-M} = e^{-2\pi^2\langle u^2\rangle/d_H^2}$. Using a Debye temperature of 365 K the thermal vibrational amplitude in bulk Ge is 0.068 Å. Since the Ge films are buried under Si and presumably strained, the atomic vibrational amplitudes are not expected to be significantly different than 0.068 Å.

In a previous XSW study (that combined the (0 0 4) and (0 0 8) reflections) the thermal vibrational amplitude for Ge buried in Si(0 0 1) was determined to be $\langle u^2\rangle^{1/2} = 0.08 \pm 0.02$ Å [20].

To model lower than expected values for Ge coherent fraction for the samples with Bi we will include a static DW factor, in addition to the thermal Debye–Waller factor. This static DW factor will replace the ordered fraction, C, in Eq. (2). For planes of index $\boldsymbol{H}$, if this displacement field has a symmetric distribution along the $\boldsymbol{H}$ direction then the measured coherent position will not change. We will assume a Gaussian distribution about the expected Ge atomic position. The static DW factor, which is then the $\boldsymbol{H}$th Fourier component of this distribution, is written as $\mathrm{e}^{-W} = \mathrm{e}^{-2\pi^2\sigma_H^2/d_H^2}$, where σ_H is the Gaussian width. Note that this is identical in form to the thermal DW factor. Without performing XSW measurements at different temperatures one cannot unambiguously separate these two contributions. With the inclusion of the static DW factor, the equation for modeling the coherent fraction becomes:

$$f_H = \mathrm{e}^{-W}\mathrm{e}^{-M}\frac{1}{N}\frac{\sin(N\pi\delta_H^F)}{\sin(\pi\delta_H^F)}. \quad (4)$$

Using a bulk Ge vibrational amplitude of 0.068 Å in the above equation, the calculated σ_{004} and σ_{022} values from our measured values of the coherent fraction for different coverages of Ge are listed in Table 1. The values of σ_{004} and σ_{022} increase with Ge coverage and the disorder appears to be isotropic within experimental error.

Table 1
The calculated widths (σ_H) for static displacements for various coverages (Θ) of Ge based on a model that includes a static Debye–Waller factor (see Eq. (4))

Θ (ML) ±0.1 ML	σ_{004} (Å) ±0.03 Å	σ_{022} (Å) ±0.03 Å
1.6	0.09	0.05
1.7	0.09	0.07
3.0	0.14	0.18
3.4	0.13	0.21
4.6	0.25	0.23
7.1	0.29	0.28
10.0	0.42	0.43

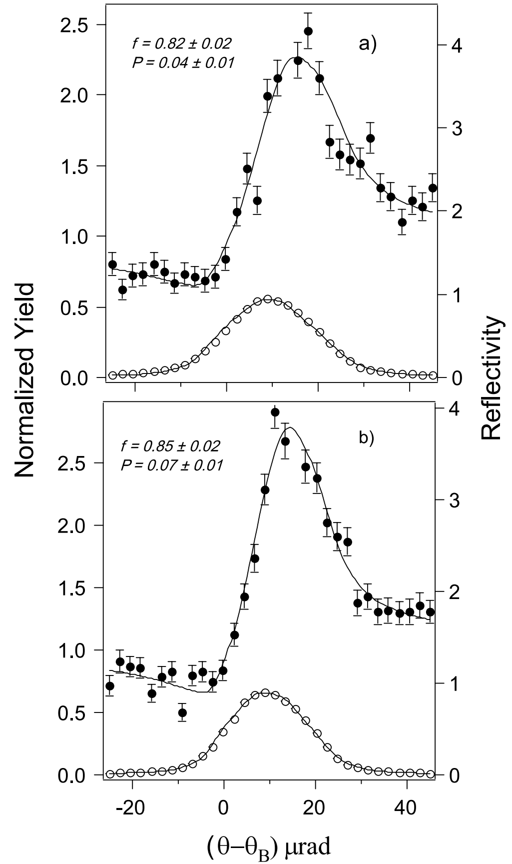

Fig. 4. (0 0 4) XSW Si cap data and fit for (a) 1.1 ML Ge with no surfactant and (b) 1.6 ML Ge with Bi as a surfactant. The data was taken at 8.0 keV.

Fig. 4 shows the Si capping layer XSW data for two samples where the combined XSW and evanescent-wave emission measurements were performed. Table 2 contains the entire data set for the four samples where both Ge and Si cap XSW measurements were made. These same four samples are included in the previous Ge buried layer analysis.

4. Discussion

It is clear from the data set (Fig. 3) that while the mean positions of the Ge atoms are consistent with a strained tetragonally distorted lattice, there exists an appreciable spread about this mean Ge

Table 2
Ge and Si values for (0 0 4) coherent position and coherent fraction for samples where combined XSW and evanescent-wave emission measurements were performed

Θ (ML) $\pm$ 0.1 ML	Bi surfactant?	$f_{004}^{Ge} \pm 0.02$	$f_{004}^{Si} \pm 0.02$	$P_{004}^{Ge} \pm 0.01$	$P_{004}^{Si} \pm 0.01$
1.1	No	0.72	0.82	0.03	0.04
1.6	Yes	0.82	0.85	0.06	0.07
3.0	Yes	0.70	0.44	0.12	0.18
3.4	Yes	0.70	0.43	0.14	0.21

position; especially at coverages above 4 ML. Specular reflectivity experiments that we performed on the same samples [13] confirmed that the Ge/Si substrate interfaces are abrupt and that the Ge/Si cap interface roughness is quite low (~3.2 Å) for the 7.1 ML sample, but much higher (~11.5 Å) for the 10 ML Ge sample. In the same study [13] in-plane grazing incidence diffraction (GIXD) measurements indicated that the onset of strain relaxation occurred between 7 and 10 ML and that the relaxation was accommodated at the Ge/Si cap interface. In the present XSW study of these same samples, 7 ML is when the P_{004} values begin to deviate from elasticity theory predictions (see Fig. 3). This likely marks the onset of growth front roughening as Ge atoms are transported to upper layer positions. This 7 ML threshold was also found by LeGoues et al. [4] using TEM for the case of arsenic as a surfactant.

As for the 1.1 ML Ge sample grown without surfactant, the measured coherent position agrees with our ideal model, while the coherent fraction is lower than predicted. Previous work on Si/Ge samples grown without surfactant at 400 °C shows that Ge will diffuse into and to the top of the Si cap layer [21,22]. Unlike our SME samples, a small amount of Ge was detected on the surface of this sample by AES after the 100 Å Si cap was deposited. Upon removal from the vacuum chamber this surface segregated Ge would expectedly oxidize into an amorphous phase. It is also likely that some fraction of the Ge will have diffused into the Si substrate [23] which further complicates the calculation of expected f_H^{Ge} and P_H^{Ge} values.

In a previous SME Si/Ge/Si(0 0 1) report [20] we examined similar structures using group VI Te as the surfactant rather than group V Bi. The samples grown with Te had f_H, as well as P_H, values that were consistent with continuum elasticity theory. The higher f_H^{Ge} values, in agreement with the predictions of an ideal-strained-pseudomorphic layer, imply that Te is more effective as a surfactant than Bi. Te and Bi surface structures on Si(0 0 1) and Ge(0 0 1) are different and this is likely related to their performance as a surfactant. The saturated Te/Si(0 0 1) and Te/Ge(0 0 1) surfaces result in a 1×1 termination whereby ~0.8 ML Te atoms adsorb at bridge sites with occasional missing Te rows to accommodate the larger Te atom [24–26]. This is in contrast to the 0.8 ML Bi-terminated surface that is $2 \times n$ with Bi dimers forming on the surface and occasional missing Bi dimer rows [15,27,28]. Recent theoretical and experimental work has proposed surfactant exchange pathways for group V atoms such as As and Sb in Ge/Si SME [29–32]. The debate continues to find the precise mechanism for surfactant action, however, some properties are agreed upon. For instance, it is agreed that the surfactant behavior is coverage dependant. The group V surfactant and oncoming Ge adatoms exchange as dimers i.e. one Ge dimer for one As or Sb dimer as opposed to single adatom exchange [33,34]. Tromp et al. [30] propose that two adjacent Ge dimers must be present to exchange with the underlying surfactant. Since Bi, like As and Sb, forms dimers on Ge(0 0 1) and Si(0 0 1) terminated surfaces, it is probable that it behaves similarly as a surfactant in terms of the diffusion pathway. Te on the other hand does not dimerize on Si and Ge, therefore, the surfactant exchange process should be simpler and with a smaller energy barrier since Ge adatoms will undergo single adatom exchange with the Te. This process is more efficient than for the group V surfactants, since fewer bonds are broken in the process. The lower activation energy for exchange

will reduce the adatom surface diffusion and increase the Ge incorporation, likely resulting in more coherent Ge film.

Due to its higher surface free energy the growth of Si on Ge is expected to be Volmer–Weber mode. It has been proposed that the use of a surfactant can change the growth mode of Si on Ge to Frank–van der Merwe [1,35]. Additionally, this surface free energy difference strongly promotes Ge segregation into and on top of the growing epitaxial layer. The Si capping layer XSW–evanescent-wave results indicate that high quality Si epitaxial layers can be grown on Ge layers to at least 2 ML in coverage. If the Ge layers are strained, the Si coherent fractions from the epitaxial silicon layer should be approximately equal to the Debye–Waller factor for Si ($D_{004} = 0.95$, $D_{022} = 0.975$). The measured values are lower than this value since the samples are removed from vacuum and a native oxide has formed on the surface (∼20 Å). Of the 100 Å of Si deposited, approximately 10 Å will be an amorphous SiO_2 phase since 45% of the native oxide thickness will have consumed some of the original Si. The Si contained in this phase will be disordered, and therefore the ideal f_{004}^{Si} for such a sample should be 0.85. The measured f_{004}^{Si} values for samples below 2 ML in are in agreement with this value. If the Ge epitaxial layer is completely strained in compression to match the Si in-plane lattice constant, then one would expect the Si cap layer to be unstrained (with a bulk-like lattice constant). To be consistent with the results for the Ge buried-layer, the P_{004}^{Si} values for the Si cap layer should be (and are) greater than the measured P_{004}^{Ge} values. As previously stated the predicted value for an ideal pseudomorphic heterostructure is $P_{004}^{\text{Si-Cap}} = 0.068 \cdot N$. This predicted value is in reasonable agreement with the results shown in Table 2 for the 1.1 ML non-SME and 1.6 ML SME samples and is in good agreement with the results for the 3.0 and 3.4 ML SME samples. This very high-resolution XSW measured phase shift (or vertical offset) in the Si cap lattice relative to the Si substrate lattice (where the XSW is generated) has a number of remarkable implications. The cap phase shift is directly attributable to the number of intervening tetragonally-strained Ge unit cells and is therefore, when combined with the Ge coverage measurement, a second measurement of the strain in the Ge film. The cap XSW results also attest to the high quality of the epitaxy in the strained Ge layer and in the unstrained Si cap. Unlike cross-sectional HRTEM, this registration is being averaged over lateral dimensions measured in millimeters (i.e., the X-ray beam foot-print).

The Si coherent fractions for the 3.0 and 3.4 ML Ge samples are significantly lower than the 0.85 ideal values and suggest that a relatively significant fraction of the Si is disordered in these samples. These samples have, σ_{004}^{Ge} values that are 0.14 and 0.13 Å, respectively. The high σ_{004}^{Ge} values for these samples indicate that a rough Ge surface is potentially present which would lead to a poor quality template for the Si epitaxial layer. While Bi has successfully improved the quality of the Ge epitaxy it appears to have not succeeded in providing a sufficiently high enough quality Ge layer that is suitable for Si epitaxy for Ge coverage $\geqslant 3$ ML. Defects such as Ge dimer vacancies are likely present in these samples during growth and curb the ability to achieve 2-D step flow growth for the Si. Diffraction and reflectivity studies support the theory that a significant number of defects can exist in cap layers in samples similar to ours [36]. In this study X-ray diffraction measured a thinner Si layer in the cap than measured by reflectivity. Since low-angle reflectivity is sensitive to only changes in electron density, it is insensitive to the crystallinity of the epitaxial layers. The lower thickness measured by diffraction can then be attributed to defects. A similar study with our samples has been performed and will appear elsewhere [37]. A recent STM study [38] comparing the roughness of homoepitaxial Si/Si(0 0 1) for samples grown with surfactant (Sb) concluded that the introduction of Sb inhibited Si attachment on step edges resulting in the creation of 3-D islands and a rough surface. It is possible that Bi, like Sb promotes a similar effect in our silicon cap growth and that growth front roughening is therefore responsible for lowering our coherent fractions. However, our 1.6 ML Ge sample prepared with Bi has a relatively high $f_{004}^{\text{Si-cap}} = 0.85$ and this sample was

prepared using identical conditions to the other two thicker samples other than total Ge coverage. This would suggest that Bi, unlike Sb, promotes step flow growth of Si/Si and Si/Ge.

5. Conclusions

We have demonstrated that Bi is effective in promoting 2-D growth and preventing segregation in Ge/Si(0 0 1) epitaxy. The degree to which Bi would be successful in creating suitable Si/Ge superlattices is not clear as we find a significant amount of static disorder in the buried Ge layer. This suggests that defects are present in these layers when grown thicker than 3 ML. Similar XSW work using Te as a surfactant [20] suggests that Te is a more effective surfactant, which is likely due to its ability to form more highly-passivated Si(0 0 1) and Ge(0 0 1) surfaces. We also demonstrated how the combined XSW–evanescent-wave measurement can be used as an independent means for characterizing the strain and crystallinity of the heteroepitaxial layers.

Acknowledgements

We would like to thank D.L. Marasco and D.A. Walko for their help in setting up the XSW experiments. We are also grateful to P. Baldo at ANL for RBS measurements. The work was supported by the US Department of Energy/BES under contract W-31-109-Eng-38 to ANL and by the National Science Foundation under contracts DMR-0076097 and DMR-9973436, and by the State of Illinois under contract IBHE HECA NWU 96.

References

[1] M. Copel, M.C. Reuter, E. Kaxiras, R.M. Tromp, Phys. Rev. Lett. 63 (1989) 632.
[2] M. Horn von Hoegen, B.H. Muller, A. Alfalou, M. Henzler, Phys. Rev. Lett. 71 (1993) 3170.
[3] M. Asai, H. Ueba, C. Tatsuyama, J. Appl. Phys. 58 (1985) 2577.
[4] F.K. LeGoues, M. Copel, R.M. Tromp, Phys. Rev. B 42 (1990) 11690.
[5] X.W. Lin, Z. Lilientalweber, J. Washburn, E.R. Weber, A. Sasaki, A. Wakahara, T. Hasegawa, J. Vac. Sci. Technol. B 13 (1995) 1805.
[6] A.A. Williams, J.M.C. Thornton, J.E. Macdonald, R.G. Vansilfhout, J.F. van der Veen, M.S. Finney, A.D. Johnson, C. Norris, Phys. Rev. B 43 (1991) 5001.
[7] H.J. Osten, J. Klatt, G. Lippert, B. Dietrich, E. Bugiel, Phys. Rev. Lett. 69 (1992) 450.
[8] D.J. Eaglesham, F.C. Unterwald, D.C. Jacobson, Phys. Rev. Lett. 70 (1993) 966.
[9] A. Kawano, I. Konomi, H. Azuma, T. Hioki, S. Noda, J. Appl. Phys. 74 (1993) 4265.
[10] K. Sakamoto, K. Kyoya, K. Miki, H. Matsuhata, T. Sakamoto, Jpn. J. Appl. Phys. 32 (1993) 204.
[11] M. Katayama, T. Nakayama, M. Aono, C.F. McConville, Phys. Rev. B 54 (1996) 8600.
[12] P.F. Lyman, M.J. Bedzyk, Appl. Phys. Lett. 69 (1996) 978.
[13] W. Rodrigues, O. Sakata, T.L. Lee, D.A. Walko, D.L. Marasco, M.J. Bedzyk, J. Appl. Phys. 88 (2000) 2391.
[14] T. Schmidt, J. Falta, G. Materlik, J. Zeysing, G. Falkenberg, R.L. Johnson, Appl. Phys. Lett. 74 (1999) 1391.
[15] C. Park, R. Bakhtizin, T. Hashizume, T. Sakurai, Jpn. J. Appl. Phys. 32 (1993) 528.
[16] J. Zegenhagen, Surf. Sci. Rep. 18 (1993) 199.
[17] R.S. Becker, J.A. Golovchenko, J.R. Patel, Phys. Rev. Lett. 50 (1983) 153.
[18] T.L. Lee, Y. Qian, P.F. Lyman, J.C. Woicik, J.G. Pellegrino, M.J. Bedzyk, Physica B 221 (1996) 437.
[19] J. Hornstra, W.J. Bartels, J. Cryst. Growth 44 (1978) 513.
[20] B.P. Tinkham, D.A. Walko, D.M. Goodner, M.J. Bedzyk, Phys. Rev. B 67 (2003) 035404.
[21] P.C. Zalm, G.F.A. van de Walle, D.J. Gravesteijn, A.A. Vangorkum, Appl. Phys. Lett. 55 (1989) 2520.
[22] K. Nakagawa, M. Miyao, J. Appl. Phys. 69 (1991) 3058.
[23] B.P. Uberuaga, M. Leskovar, A.P. Smith, H. Jonsson, M. Olmstead, Phys. Rev. Lett. 84 (2000) 2441.
[24] N. Takeuchi, Surf. Sci. 426 (1999) 433.
[25] O. Sakata, P.F. Lyman, B.P. Tinkham, D.A. Walko, D.L. Marasco, T.L. Lee, M.J. Bedzyk, Phys. Rev. B 61 (2000) 16692.
[26] P.F. Lyman, D.L. Marasco, D.A. Walko, M.J. Bedzyk, Phys. Rev. B 60 (1999) 8704.
[27] G.E. Franklin, S. Tang, J.C. Woicik, M.J. Bedzyk, A.J. Freeman, J.A. Golovchenko, Phys. Rev. B. 52 (1995) R5515.
[28] Y. Qian, M.J. Bedzyk, P.F. Lyman, T.-L. Lee, S. Tang, A.J. Freeman, Phys. Rev. B 54 (1996) 4424.
[29] B.D. Yu, A. Oshiyama, Phys. Rev. Lett. 72 (1994) 3190.
[30] R.M. Tromp, M.C. Reuter, Phys. Rev. Lett. 68 (1992) 954.
[31] M. Jiang, X. Zhou, B. Li, P. Cao, Phys. Rev. B 60 (1999) 8171.
[32] M.A. Boshart, A.A. Bailes, L.E. Seiberling, Phys. Rev. Lett. 77 (1996) 1087.

[33] Y.-J. Ko, J.-Y. Yi, S.-J. Park, E.-H. Lee, K.J. Chang, Phys. Rev. Lett. 76 (1996) 3160.
[34] A.A. Bailes, M.A. Boshart, L.E. Seiberling, Nucl. Instrum. Meth. B 136–138 (1998) 804.
[35] M.E. Gonzalez-Mendez, N. Takeuchi, Surf. Sci. 441 (1999) 897.
[36] D. Bahr, J. Falta, G. Materlik, B.H. Muller, M. Horn von Hoegen, Physica B 221 (1996) 96.
[37] B.P. Tinkham, W. Rodrigues, D.A. Walko, M.J. Bedzyk, unpublished.
[38] G.G. Jernigan, P.E. Thompson, Thin Solid Films 380 (2000) 114.